



Modeling hydration properties and temperature developments of early-age concrete pavement using calorimetry tests

Qinwu Xu^{a,*}, J. Mauricio Ruiz^{a,1}, Jiong Hu^{b,2}, Kejin Wang^{c,3}, Robert O. Rasmussen^{a,1}

^a The Transtec Group, Inc., 6111 Balcones Dr., Austin, TX 78731, USA

^b Department of Engineering Technology, Texas State University - San Marcos, 601 University Drive, San Marcos, TX 78666, USA

^c Civil and Environmental Engineering, Iowa State University, Ames, IA 50011, USA

ARTICLE INFO

Article history:

Received 28 May 2010

Received in revised form 1 September 2010

Accepted 2 September 2010

Available online 15 September 2010

Key words:

Concrete

Calorimetry

Hydration

Analytical models

Temperature

ABSTRACT

This research aims to evaluate the calorimetry tests for characterizing cement hydration properties and predicting temperature developments of the early-age Portland cement concrete pavement (PCCP). Analytical models are studied to simulate hydration properties, using the measured heat evolution data from both the isothermal and semi-adiabatic tests. HIPERPAV III[®] engineering software with these analytical models embedded is used to predict temperature developments of the early-age PCCP. Results show that the maximum hydration time parameter τ corresponds to the maximum activation energy E_a . Semi-adiabatic tests result in a lower hydration shape parameter β yet a higher hydration time parameter τ than isothermal tests. As results, the simulated degree of hydration based on semi-adiabatic tests is higher at the early hours, but lower at later hours compared to that based on isothermal tests. This effect is also reflected from the simulated temperature developments of the early-age PCCP. Three engineering projects in this research show that predicted temperatures of the PCCP using hydration parameters determined from semi-adiabatic tests better match actual measurements than that from isothermal tests.

© 2010 Elsevier B.V. All rights reserved.

1. Introduction

Cement hydration plays a critical role in the temperature development of early-age concrete due to the heat generation [1,2]. It also has significant effects on material properties and performances at early age, including material strengths [3,4], critical stresses [5], and distresses like cracking [6,7]. Therefore, it is essential to capture the hydration property and temperature development of concrete at early age to prevent premature failures.

Calorimetric tests, including the isothermal, semi-adiabatic and full-adiabatic tests, have been used to capture the hydration properties and early-age properties of cement concrete. Isothermal test was performed under a constant temperature to measure the heat generation rate. Full-adiabatic test was conducted under sealed condition without heat exchange with environment to measure temperature developments. However, “heat isolation” from environment in the full-adiabatic test is practically difficult to obtain

due to the equipment limitations. Alternatively, the semi-adiabatic test is used, which allows partial heat exchange of concrete with the surrounding environment through heat transfer. Calorimeter test has been used to characterize the hydration properties of cement and blended cements such including the alkali-slag cements [8] and calcium aluminate cement (CAC) [9]. Hydration properties determined from calorimetry tests include the activation energy [10], time of set [11], and hydration curve parameters [12], etc. Calorimetry tests are also used to study material design and the influences of material components on early-age properties. For example, calorimetry studies show that Portland cement and CAC ratio play a critical role in heat profile and early-age strength development [9], decreasing w/c ratio increases the peak temperature of semi-adiabatic hydration (when $w/c \geq 0.38$) and reduces degree of achievable hydration [13], adding fly ash and water reducer delays hydration and reduces thermal stress (isothermal tests) [12], drying (removal of water) reduces hydration rate and thermal power [14], blending with fly ash, ground-granulated slag, and silica fume has slowed down the pozzolanic reaction [15], etc.

It is believed that isothermal test has advantages over adiabatic test, due to the following: it directly measures the heat generation rate; it does not require the knowledge of heat capacity of material for determining degree of hydration (DOH); and the modern isothermal calorimeter is very reliable and requires less calibration [16]. The disadvantages of isothermal test may be that only

* Corresponding author. Tel.: +1 512 451 6233; fax: +1 512 451 6234.

E-mail addresses: qinwu.xu@yahoo.com (Q. Xu), jiong.hu@txstate.edu (J. Hu), kejinhw@iastate.edu (K. Wang).

¹ Tel.: +1 512 451 6233; fax: +1 512 451 6234.

² Tel.: +1 512 245 6328; fax: +1 512 245 3052.

³ Tel.: +1 515 294 2152; fax: +1 515 294 8216.

small specimens such as cement and mortar samples can be used [16]. Cement and concrete hydration property has been characterized using hydration parameters including the activation energy E_a , hydration curve parameters (ultimate hydration degree α_u , hydration shape parameter β , and hydration time parameter τ). These parameters can be determined from calorimetric tests, and then be used to simulate the DOH and temperature developments in the early-age PCCP.

However, it is still not very clear which calorimetry test would better or more accurately characterize the early-age properties and predict temperature developments of concrete. Literature review shows that very limited researches have compared these calorimetric test methods in determining hydration properties and predicting temperature developments of the early-age concrete.

Accordingly, this paper aims to evaluate the calorimetric test methods to ascertain hydration characteristics for predicting temperature developments of the early-age PCCP. Isothermal and semi-adiabatic tests were conducted on three different mix designs of cement mortars and concretes. Analytical models are studied for modeling hydration parameters. By utilizing these modeled hydration parameters determined from calorimetry tests, temperature developments of the early-age PCCP were simulated using the HIPERAPV III[®] engineering software. Temperatures of the PCCP were also measured in field to validate modeling results and evaluate calorimetry tests.

2. Construction and materials design

Portland cement concrete pavements (PCCP) were constructed in three highway sites as follows: Atlantic of Iowa, Alma Center of Wisconsin, and Ottumwa of Iowa, all in the United States of America. The PCCP slab has a thickness of 20.3 cm (8 in.) for the Atlantic, and a thickness of 30.5 cm (12 in.) for both Alma Center and Ottumwa. These PCCP slabs have a width of 4.88 m (16 ft), and a length of 5.49 m (18 ft). Type IP (F), Type I/II GU, and Type ISM cements were used for the PCCP constructed in Atlantic, Alma Center, and Ottumwa, respectively. Class C fly ashes (FA) and lignosulfonate-based Type D water reducers were used in all these highway projects. The oxide compositions of cements and fly ashes were measured using the X-ray fluorescence (XRF) method, with results summarized in Table 1. The cement mortar and concrete mixture designs are detailed in Tables 2a and 2b.

3. Experimental program

3.1. Isothermal calorimetry test

Isothermal calorimetry test was performed on cement mortar to measure the heat evolution with time, as shown in Fig. 1. It should

Table 2a

Mixture design: concrete mixture.

Site	Cement (kg/m ³)	Fly ash (kg/m ³)	Coarse aggregate (kg/m ³)	Int. aggregate (kg/m ³)	Sand (kg/m ³)	Water (kg/m ³)	AEA (ml/100 kg)	WR (ml/100 kg)
Atlantic	262	65	926	162	777	131	20	261
Alma center	265	67	1083	0	813	149	65	209
Ottumwa	263	66	1095	0	766	132	20	261

Table 2b

Mixture design: mortar mixture.

Site	Cement (kg/m ³)	Fly ash (kg/m ³)	Int. aggregate (kg/m ³)	Sand (kg/m ³)	Water (kg/m ³)	AEA (ml/100 kg)	WR (ml/100 kg)
Atlantic	262	65	162	777	131	20	261
Alma Center	265	67	0	813	149	65	209
Ottumwa	263	66	0	766	132	20	261

Table 1

Oxide composition of cement and fly ash (unit: %).

	Atlantic, IA		Alma Center, WI		Ottumwa, IA	
	Cement	Fly ash	Cement	Fly ash	Cement	Fly ash
CaO	49.34	26.20	63.09	25.60	58.79	28.80
SiO ₂	29.64	34.90	20.78	36.30	23.72	31.60
Al ₂ O ₃	8.20	20.10	4.74	19.10	5.22	16.20
Fe ₂ O ₃	3.31	5.78	3.15	5.26	2.77	6.03
Na ₂ O	0.30	1.72	0.07	1.83	0.16	3.21
K ₂ O	0.73	0.42	0.78	0.47	0.56	0.32
MgO	3.08	4.63	2.35	5.29	4.30	6.81
SO ₃	3.30	2.27	2.75	1.93	2.95	3.13
P ₂ O ₅	0.10	1.01	0.08	1.03	0.10	1.02
TiO ₂	0.51	1.64	0.24	1.53	0.38	1.24
SiO	0.12	0.42	0.11	0.44	0.04	0.51
Mn ₂ O ₃	0.07	0.05	0.07	0.03	0.49	0.02
LOI	1.29	0.38	1.78	0.36	0.51	0.30

be noted that only small samples like cement paste or mortar specimens can be used in isothermal test.

3.2. Semi-adiabatic calorimetry test

The semi-adiabatic tests were performed on the concrete mixture samples with the IQ drum device shown in Fig. 1 to measure the temperature developments. The computer program also converts the temperatures from semi-adiabatic tests to that at the full-adiabatic conditions by accounting for the lost heat to the environment.

3.3. Field measurements of PCCP temperatures

The information of field concrete mixing and construction were presented in Table 3, which are essential parameter inputs for PCCP temperature prediction as discussed later. Temperatures of the field PCCP were measured using temperature sensors (ibutton) after casting concrete mixtures in construction. A stick with three ibuttons was inserted into the pavement right after paving, with the first one placed at 25 mm (1 in.) below the surface, the second one in the slab middle, and the third one at 25 mm (1 in.) above the slab bottom. The stick was placed one foot from the edge of the pavement to avoid the edge effect due to the heat exchange between slab and environment. As shown in Fig. 2, cables were running outside from the pavement in order to retrieve temperature data after paving.

4. Hydration parameters

Analytical models are studied to determine hydration parameters using the measured calorimetric test data of heat evolution.

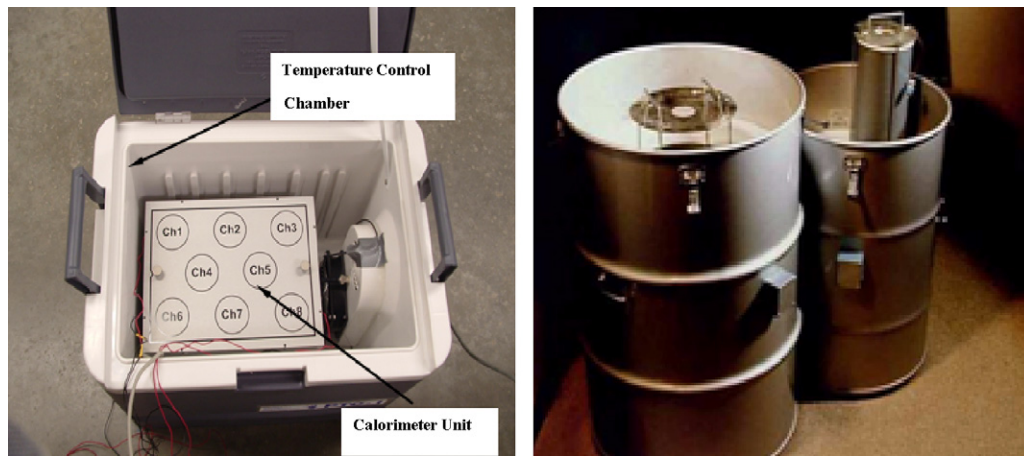


Fig. 1. Isothermal (left) and semi-adiabatic (right) test devices.

Table 3
Field concrete mixing and construction.

Highway site	Date	Mixing time	Subbase temp		Concrete temp (F)	Dump time	Paving time	Finishing time	Curing time	Sawing time	
			Infrared (F)	Probe (F)						Time	h
Atlantic	2007/6/27	12:38	121.2	97.9	86.7	13:02	13:14	13:16	14:12	22:57	10:32
Alma Center	2007/7/18	9:23	88.7	82.6	74.7	9:27	9:31	9:33	0:11	19:40	10:28
Ottumwa	2007/7/24	12:40	90.6	91.3	87.6	12:48	13:02	13:09	13:34	21:05	8:42

4.1. Equivalent age

“Equivalent age” is a common concept used in concrete industry to describe the maturity of concrete material. The mostly common expression for the equivalent age, t_e , was proposed by Hansen and Pedersen [17] as follows:

$$t_e = \sum e^{-(E_a/R)((1/T_c)-(1/T_r))} \cdot \Delta t \quad (1)$$

where T_c is the temperature of concrete (K), T_r is the reference temperature (294.25K), E_a is activation energy, and R is universal gas constant (8.3144 J/mol/°C).

Activation energy E_a (J) is the energy required to be overcome for hydration of cement. E_a can be determined from the Arrhenius equation [18,19] as follows:

$$P(T) = Ae^{-(E_a/RT)} \quad (2)$$

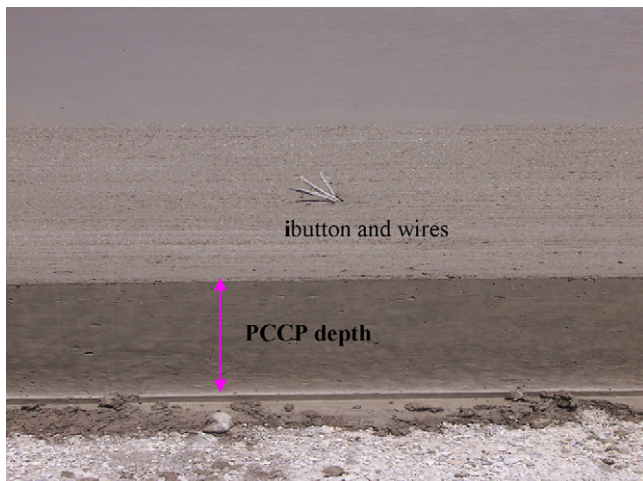


Fig. 2. Concrete pavement and temperature measurement.

where $P(T)$ is the heat generation rate of isothermal test, A is the pre-exponential factor, T is temperature (K), and R is universal gas constant. This equation shows that the logarithmically scaled $P(T)$ has a linear relationship with T inverse, with a slope of E_a/R . Thus, E_a can be determined from this linear relationship using isothermal calorimetry test data from several different temperatures.

4.2. Degree of hydration (DOH)

The well-known exponential model is used to express the DOH [20,21] as follows:

$$\alpha(t_e) = \alpha_u \cdot e^{-[\tau/t_e]^\beta} \quad (3)$$

where α_u represents the ultimate DOH, a material-dependent parameter. τ is the hydration time parameter (hrs), and a larger τ implies a larger delay for hydration. β is the hydration shape parameter, which primarily represents the slope of the major linear portion of the hydration–time relationship as shown in Fig. 3. A

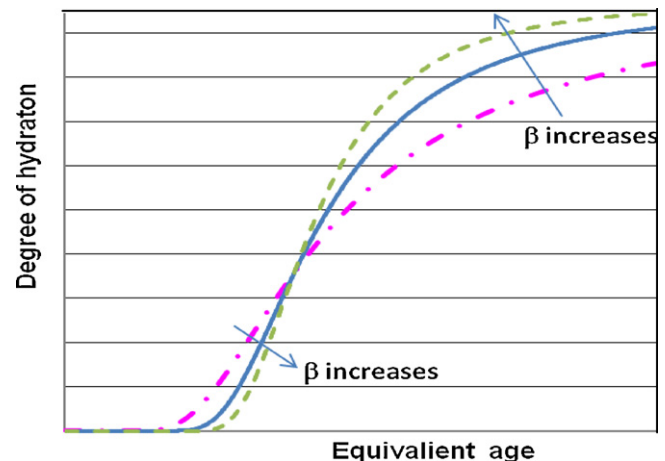


Fig. 3. Influence of β on the degree of hydration (see Ref. [22]).

larger β implies a higher hydration rate of that linear portion while a lower hydration rate at the beginning of hydration time [22,23]. From Eq. (3), it can also be indicated that a greater β results in a lower hydration rate when τ is smaller than t_e .

4.3. Hydration curve parameters determined from isothermal test

Using the isothermal test data, the DOH at time t can be expressed as a ratio of the heat evolved $H(t)$ at time t over the total or ultimate heat H_u of the material [24,25]:

$$\alpha(t) = \frac{H(t)}{H_u} \quad (4)$$

The time t can be converted to the equivalent age t_e using Eq. (1), and then the DOH in Eq. (4) is re-expressed as follows:

$$\alpha(t_e) = \frac{H(t_e)}{H_u} \quad (5)$$

The total heat H_u is dependent on material composition and amount, and type of supplementary cementing materials (SCMs). H_u can be calculated as follows [22,23]:

$$H_u = H_{cem} \cdot P_{cem} + 461P_{slag} + 1800P_{FA-CaO} \cdot P_{FA} \quad (6)$$

where P_{slag} is the mass ratio of slag over total cementitious content, P_{FA} is the mass ratio of fly ash over total cementitious content,

P_{FA-CaO} is the mass ratio of CaO in fly ash over the total fly ash content, and P_{cem} is the mass ratio of cement over the total cementitious content.

H_{cem} is the total heat of cement hydration (J/g), which can be determined as follows [22,23]:

$$H_{cem} = 500P_{C_3S} + 260P_{C_2S} + 866P_{C_3} + 420P_{C_4AF} + 624P_{SO_3} + 1186P_{Free\ Ca} + 850P_{MgO} \quad (7)$$

where P is the mass ratio of the component to the total cement content, which is determined from the material chemical composition test according to the ASTM C150 “Standard Specification for Portland Cement” (see results in Table 1).

The hydration curve parameters (α_u , β , and τ) can be determined through curve fitting by minimizing the DOH difference between measurements (using Eq. (5)) and simulation results (using Eq. (3)).

4.4. Hydration curve parameters from adiabatic tests

Hydration curve parameters can also be determined from the adiabatic test using the temperature–time history data.

Substitute Eq. (3) to Eq. (5), the generated heat of concrete at the equivalent age t_e can be determined as follows:

$$H(t_e) = \alpha(t_e) \cdot H_u = \alpha_u \cdot e^{-[\tau/t_e]^\beta} \cdot H_u \quad (8)$$

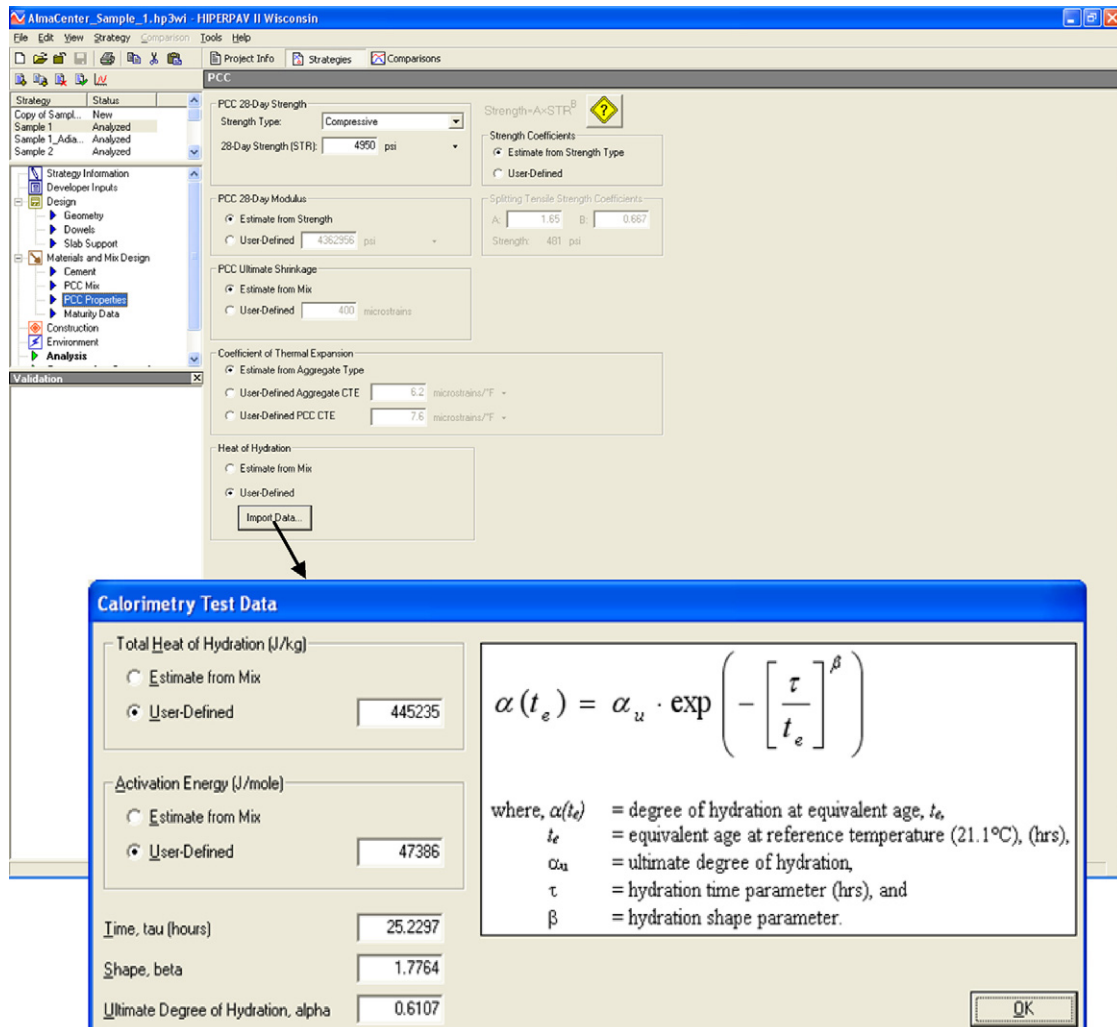


Fig. 4. HIPERPAV III® interface.

Then the heat generation rate (W/m³) can be determined as follows:

$$P(t) = \frac{dH(t_e)}{dt} = \frac{dH(t_e)}{dt_e} \frac{dt_e}{dt} \quad (9)$$

By substituting Eq. (8) into Eq. (9), heat generation rate $P(t_e)$ at t_e can be derived as follows:

$$\frac{dH(t_e)}{dt_e} = H_u \cdot \alpha_u \cdot e^{-[\tau/t_e]^\beta} \cdot \frac{\beta}{t_e} \cdot \left(\frac{\tau}{t_e}\right)^\beta \quad (10)$$

Meanwhile, from Eq. (1) the derivative of equivalent age t_e to time t can be achieved as follows:

$$\frac{dt_e}{dt} = e^{-(E_a/R)((1/T_c)-(1/T_r))} \quad (11)$$

Substitute Eqs. (10) and (11) into Eq. (9), the heat generation rate $P(t)$ at time t is determined as follows:

$$P(t) = H_u \cdot \alpha_u \cdot e^{-[\tau/t_e]^\beta} \cdot \frac{\beta}{t_e} \cdot \left(\frac{\tau}{t_e}\right)^\beta e^{-(E_a/R)((1/T_c)-(1/T_r))} \quad (12)$$

Using Eq. (12), the heat rise at a time step (from time t_i to time t_{i+1}) can be determined as follows:

$$\Delta H(t) = \int_{t_i}^{t_{i+1}} P(t) \quad (13)$$

Thus, the temperature rise at each time step can be determined as follows:

$$\Delta T = \frac{\Delta H(t)}{C_c} \quad (14)$$

where C_c is the specific heat of cementitious material.

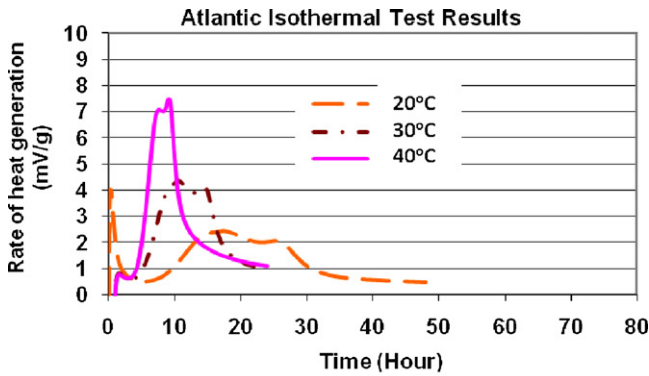
Therefore, the temperature accumulated up to time t is attained as follows:

$$T(t) = \int_{t_0}^t \frac{\Delta H(t)}{C_c} \quad (15)$$

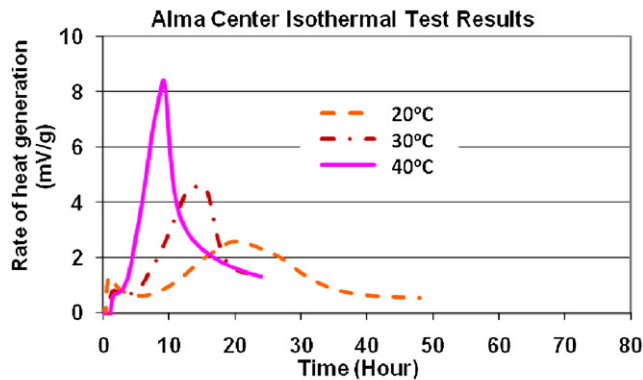
Here a chi-square statistics χ^2 is used, as the sum of the temperature differences between predictions and measurements over the measurement variance:

$$\chi = \sum_{i=1}^N \left[\frac{(|T_m| - |T_p|)^2}{\sigma_{T_m}^2} \right] \quad (16)$$

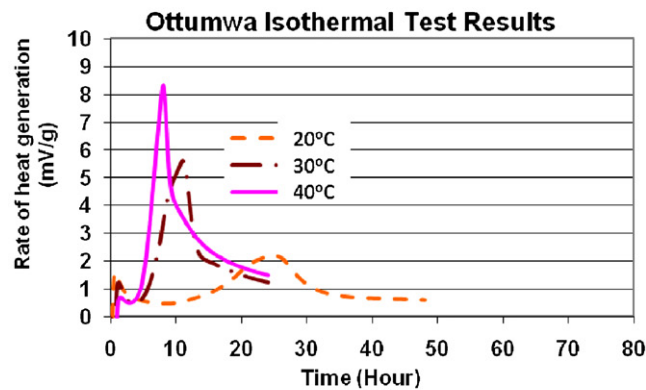
where T_m is the measured temperature, T_p is the predicted temperature, σ_{T_m} is the standard deviation of the measured temperatures, N is the measured data point number.



(a) Rates of heat generation of Atlantic concrete from isothermal tests

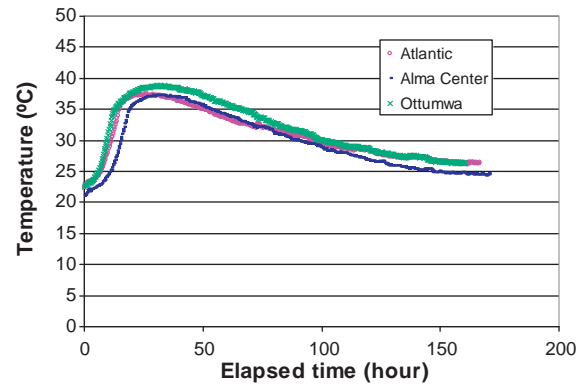


(b) Rates of heat generation of Alma Center concrete from isothermal tests

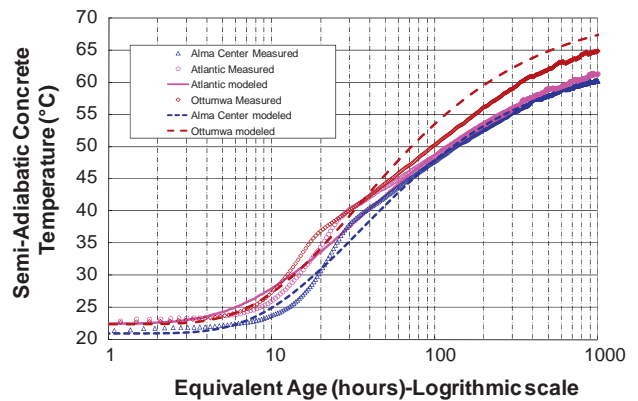


(c) Rates of heat generation of Ottumwa concrete from isothermal tests

Fig. 5. Heat generation of Isothermal tests.



(a) Semi-adiabatic tested temperatures



(b) Converted full-adiabatic temperature and simulations at equivalent age

Fig. 6. Measured PCCP temperatures from semi-adiabatic test and full-adiabatic conversion and simulation.

As T_m and T_p are considered independent and following the normal distribution, χ^2 would follow the chi-square distribution with N degrees of freedom. χ^2 is minimized to achieve the optimum curve fitting using the Solve function embedded in the Microsoft Excel, which returns the hydration curve parameters. The χ^2 value can also be used as a statistical index to evaluate the goodness of fit.

5. Temperature prediction using HIPERPAV III® software

With the determined hydration parameters (E_a and hydration curve parameters) and given environmental conditions, DOH and heat generation rate, and temperature developments of the early-age PCCP can be simulated. In this study, the HIPERPAV III®, an engineering software of the Federal Highway Administration (FHWA) developed by the research team [26,27], is used to predict temperature developments of the early-age PCCP. HIPERPAV® can effectively predict temperature development in the early-age PCCP as validated by previous research and engi-

Table 4a

Hydration curve parameters: calculated from isothermal test results.

Sample	Parameters	20 °C	30 °C	40 °C	Mean
Atlantic, Iowa	α_u	0.61	0.58	0.54	0.57
	β	1.70	1.94	2.24	1.96
	τ (h)	18.34	20.82	27.26	22.14
Alma Center, Wisconsin	α_u	0.61	0.63	0.60	0.61
	β	1.64	1.75	1.94	1.78
	τ (h)	20.25	26.00	29.48	25.23
Ottumwa, Iowa	α_u	0.53	0.49	0.63	0.63
	β	1.61	1.95	1.42	1.42
	τ (h)	14.21	16.62	20.42	20.42

neering practices [28,29]. The temperature model has accounted for the influences of both cement hydration and environmental conditions, and its computation algorithm is based on a finite difference method as detailed in previous research [28–30]. The most update version of HIPERPAV III® allows users to define the hydration model parameters, determined from calorimetry test data as shown in Fig. 4 [26], while the older versions estimate hydration parameters from the material chemical composition [28–30]. The required weather information during the construction period was attained from the Weather Underground Station (<http://www.wunderground.com/>).

6. Results and analysis

6.1. Heat–time and temperature–time relationships

The isothermal test results of heat evolutions (mV/g) of the three mixtures used at Atlantic, Alma Center, and Ottumwa are illustrated in Fig. 5, results showed that apparently heat generation rate is higher under higher temperature. For the Atlantic mixture, a double peak of heat generation rate is found. This is likely due to the fact that a much lower CaO content and a higher ratio of supplemental cementitious materials (SCMs) were used (see Table 1), resulting in a second and delayed hydration peak due to the slower pozzolans reaction [31,32].

The measured temperature–time relationship of the semi-adiabatic test, and converted full-adiabatic results were presented in Fig. 6 (note that it also presented the predicted temperatures and will be discussed later).

6.2. Hydration parameters

The activation energy E_a determined from the isothermal calorimetry tests for the mixtures used in the Atlantic, Alma Center, and Ottumwa projects are 43.3, 47.4, and 43.2 kJ/mol, respectively. The hydration curve parameters determined from isothermal tests are presented in Table 4a. Results show that the Alma Center mix has the highest E_a and τ value among these three mixtures, which maybe indicate that a higher E_a requires a higher energy and thus “delays” the occurrence of cement hydration (with larger τ value). Previous research has shown that generally the variation trend of τ is consistent with that of E_a [12].

Table 4b summarizes the hydration curve parameters determined from the analytical models based on the semi-adiabatic test

Table 4b

Hydration curve parameters: calculated from semi-adiabatic test.

Parameters	Atlantic field concrete	Alma Center field concrete	Ottumwa field concrete
α_u	0.66	0.63	0.69
β	0.60	0.71	0.58
τ (h)	32.50	33.29	32.28

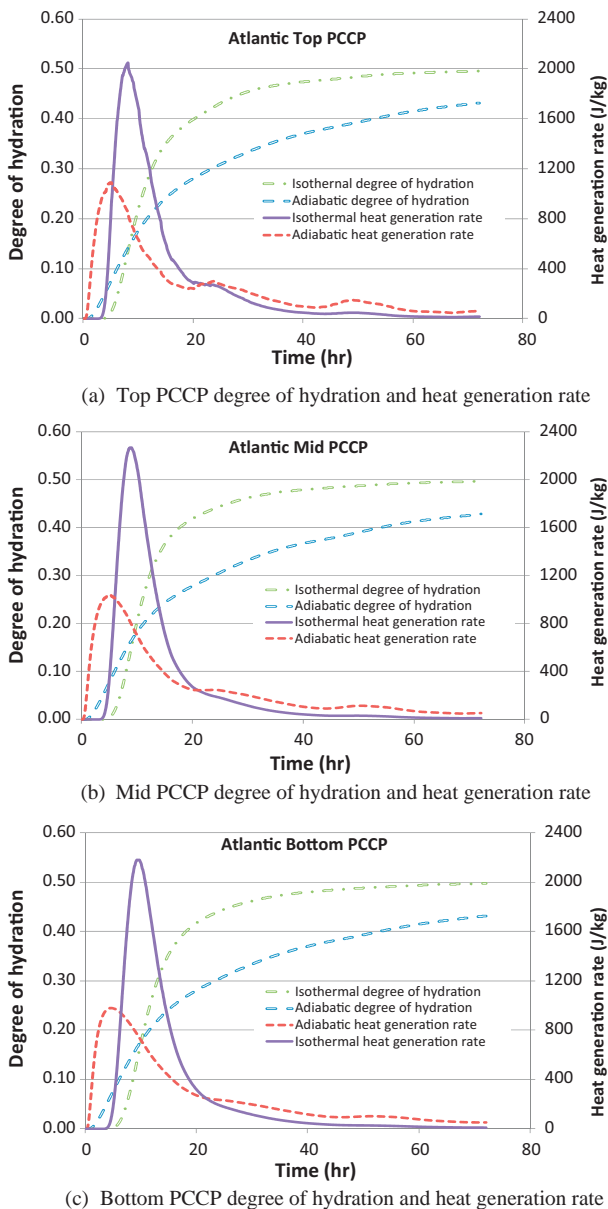


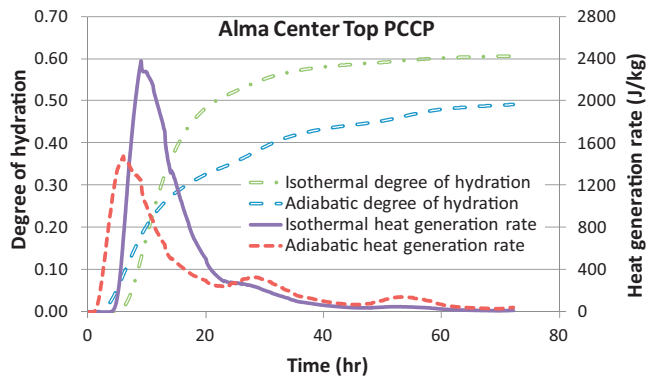
Fig. 7. Simulated degree of hydration and heat generation rate (Atlantic, IA).

data. Results also show that the Alma Center mix has greatest E_a and τ values as that of isothermal tests. It also shows that the semi-adiabatic test data result in higher τ values, while much lower β values than isothermal test data. This result may be due to the “delayed” effects of coarse aggregates used in concrete mixture for semi-adiabatic tests.

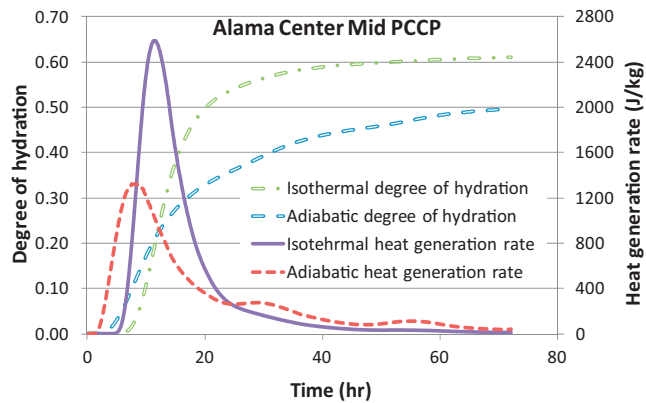
6.3. Simulated degrees of hydration and temperatures of PCCP

6.3.1. Degree of hydration and heat generation rate

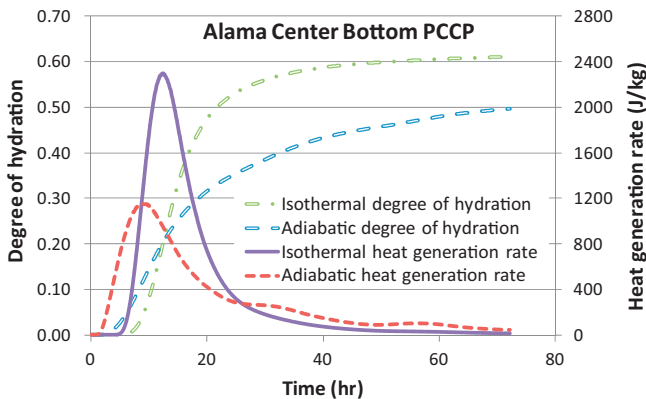
Figs. 7–9 display the simulation results of DOH and rates of heat generation for the early-age PCCP used in Atlantic, Alma Center, and Ottumwa projects, respectively. Results show that in the first several hours the simulated DOH using hydration curve parameters based on isothermal tests is lower than that based on



(a) Top PCCP degree of hydration and heat generation rate

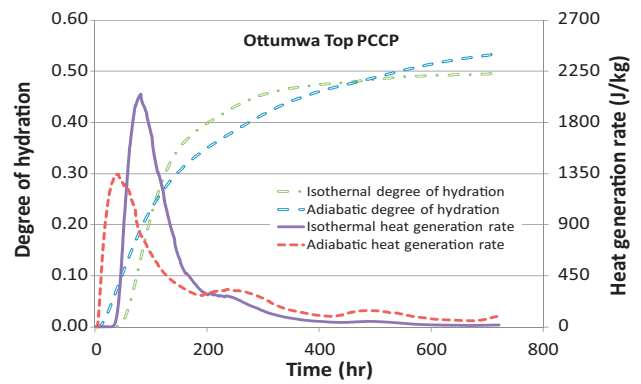


(b) Mid PCCP degree of hydration and heat generation rate

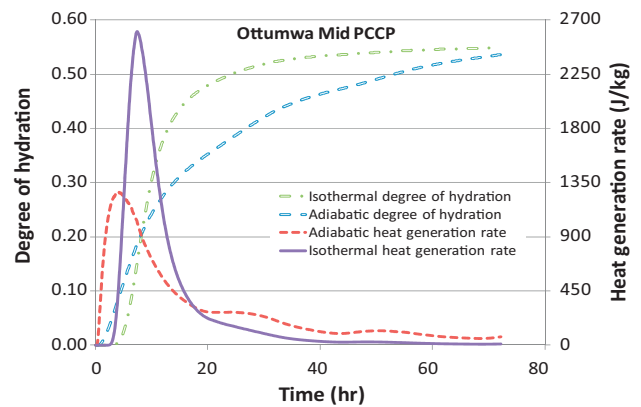


(c) Bottom PCCP degree of hydration and heat generation rate

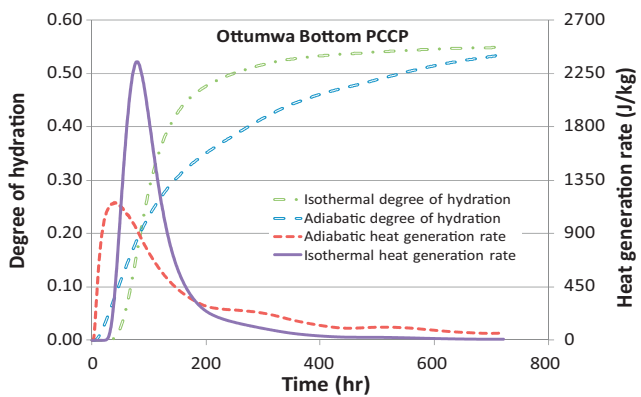
Fig. 8. Simulated degree of hydration and heat generation rate (Alma Center, WI).



(a) Top PCCP degree of hydration and heat generation rate



(b) Mid PCCP degree of hydration and heat generation rate



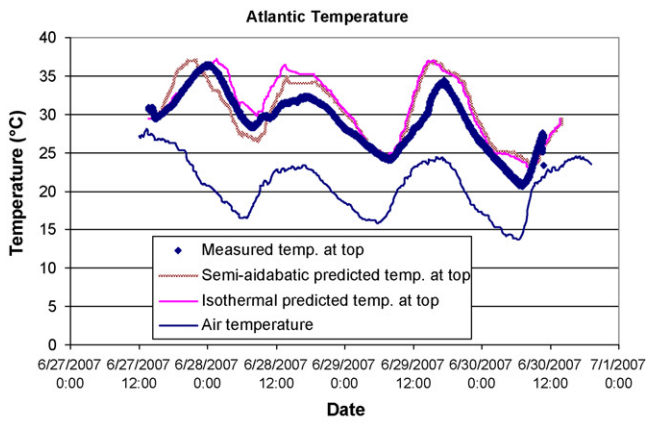
(c) Bottom PCCP degree of hydration and heat generation rate

Fig. 9. Simulated degree of hydration and heat generation rate (Ottumwa, IA).

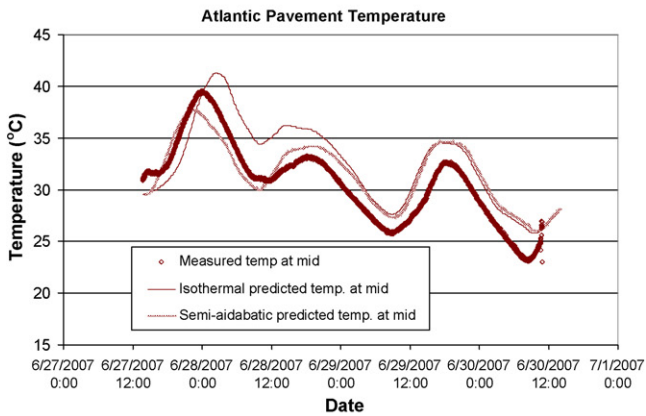
semi-adiabatic tests, but higher and increases faster in later hours. This phenomenon maybe primarily due to the higher β value determined from isothermal test, since a higher β value induces a lower DOH at the time beginning, while a greater DOH and faster increase at later hours (see Fig. 3). Meanwhile, it is noted that the DOH and heat generation rate at the top, mid, and bottom of PCCP are different especially at the early hours, which is primarily due to the influences of environmental conditions including the ambient air temperature and base layer condition. In addition, a second and third peak of DOH appears, which would be primarily due to the daily temperature cycling effect of the ambient air for the 2nd and 3rd day.

6.3.2. PCCP temperature developments

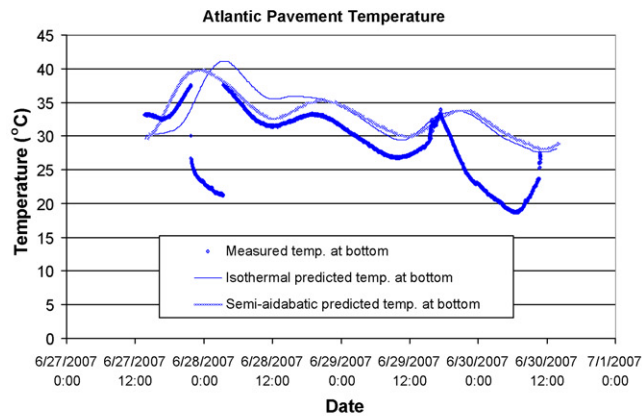
Fig. 10 presents the HIPERPAV III® simulated temperature developments at the top, mid, and bottom of the PCCP slab in the Atlantic



(a) Pavement top and ambient air



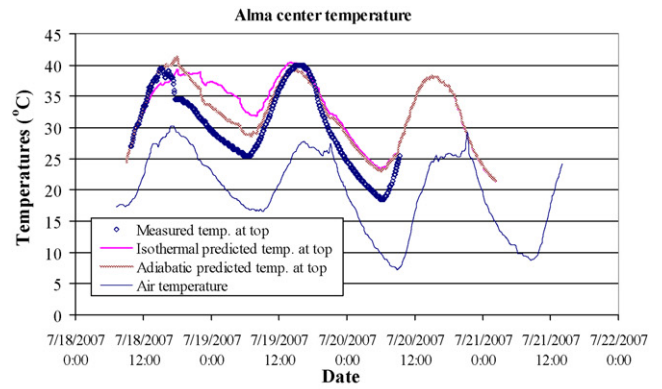
(b) Pavement mid



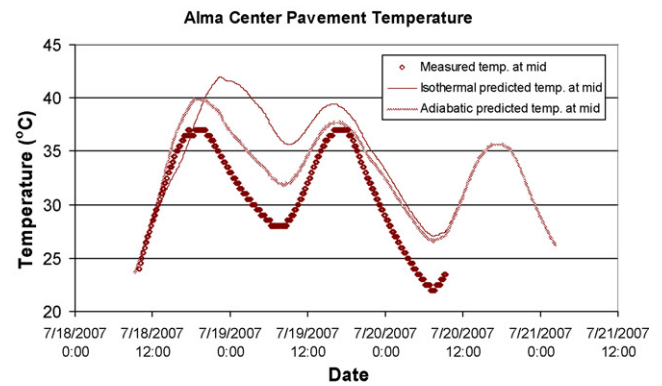
(c) Pavement bottom

Fig. 10. Predicted PCCP temperatures vs. measurements (Atlantic, IA).

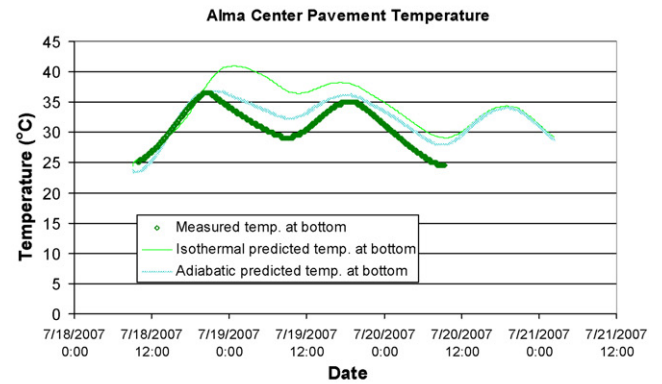
highway site, using hydration curve parameters determined from both isothermal and semi-adiabatic tests. The predicted PCCP temperatures in the Alma Center and Ottumwa sites are presented in Figs. 11–12, respectively. It is noted that for the Alma Center site, the actual pavement temperature was only monitored for the first 48 h rather than 72 h as expected due to in situ measuring issues. These figures all show that pavement temperatures increase sharply and then decrease, increase and decrease again, with three cycles for a period of 72 h (3 days). At the time beginning, temperature increases until reaching the highest peak, which is primarily attributed to the heat generation of cement hydration, although during the 1st daily cycle the air temperature is



(a) Pavement top and ambient air



(b) Pavement mid



(c) Pavement bottom

Fig. 11. Predicted PCCP temperatures vs. measurements (Alma Center).

decreasing after mixture cast. Consequently, after about 12 h, the trend of PCCP temperature variation basically follows that of air temperature variation, when temperatures of ambient air play a more important role than cement hydration. It is seen that the measured pavement temperatures at the bottom of the PCCP in Atlantic site experience a sudden drop (see Fig. 10), which might be due to some measurement error during that time period. Results also show that generally the predicted PCCP temperatures using isothermal test parameters are higher than that using the semi-adiabatic test parameters, especially during the first and second daily cycles, which is consistent with the simulated degrees of hydrations. This is likely due to their different hydration parameters of β and τ values as discussed previously. Table 5 summarizes the Chi-square goodness-of-fit statistics. Results indicate that the predicted temperatures using hydration curve parameters generated from semi-adiabatic test data better match actual PCCP temperatures than those generated from isothermal test data (with

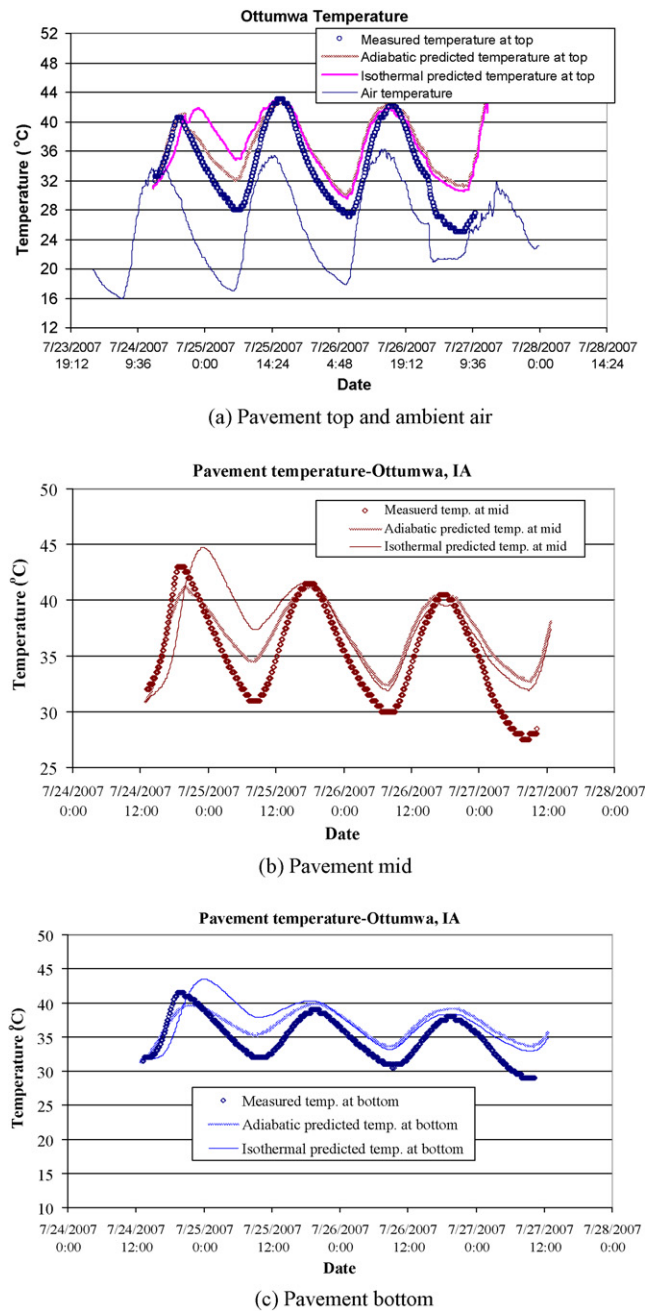


Fig. 12. Predicted PCCP temperatures vs. measurements (Ottumwa).

lower χ^2 values). This result might be due to the fact that the isothermal test is performed on the cement mortar, which may ignore the effects of coarse aggregates on the DOH of PCCP mixture.

Table 5
Chi-square statistics.

Site	Calorimetry test	<i>dF</i>	χ^2 top	χ^2 mid	χ^2 bottom
Alma Center	Isothermal	475	309.42	377.80	327.73
	Adiabatic	475	152.66	145.86	76.63
Atlantic	Isothermal	688	127.40	87.85	723.35
	Adiabatic	688	137.95	163.84	901.14
Ottumwa	Isothermal	715	238.66	233.89	724.82
	Adiabatic	715	212.56	166.41	577.01

7. Conclusions

This paper presented the experimental study and analytical models for evaluating calorimetry tests for modeling hydration properties and temperature developments of the early-age PCCP. The main findings are summarized as follows:

- The semi-adiabatic test results in a much lower hydration shape parameter β while a higher hydration time parameter τ value compared to the isothermal test. It is likely due to the fact that cement mortar instead of concrete mixtures were used in the isothermal test, which did not include the effects of coarse aggregates;
- The simulated pavement temperatures using hydration parameters generated from isothermal tests have lower values and a small delay at the early hours, but greater values and faster increase at later hours compared to that using hydration parameters generated from semi-adiabatic tests, which is consistent with the simulated degrees of hydration. This is primarily due to the greater β while lower τ values generated from the isothermal test;
- The predicted temperatures using hydration curve parameters generated from semi-adiabatic test data better match actual PCCP temperatures than those generated from isothermal test data based on test results of three projects in this research, which is likely due to that the semi-adiabatic test on concrete mixtures have accounted for the effect of coarse aggregates on the degree of hydration of PCCP. However, larger samples of tests may further validate this finding.

In the future study, models can be developed to calibrate isothermal tests on cement mortars for a higher accuracy in temperature predictions of the early-age concrete mixture, while taking other advantages of isothermal test over semi-adiabatic test.

Acknowledgements

The work presented in this paper is part of an extensive research project, "Developing a simple and rapid test for monitoring the heat evolution of concrete mixtures for both laboratory and field applications", supported by the Federal Highway Administration of the USA. The laboratory tests were performed at the National Concrete Pavement Technology Center (CP Tech Center) at Iowa State University.

References

- [1] B.F. McCullough, R.O. Rasmussen, Fast-Track Paving: Concrete Temperature Control and Traffic Opening Criteria for Bonded Concrete Overlays—Volume I: Final Report, Publication FHWA-RD-98-167, FHWA, U.S. Department of Transportation, 1999.
- [2] K. Wang, J.M. Ruiz, J. Hu, Z. Ge, Q. Xu, J. Grove, R. Rasmussen, T. Ferragut, Developing a Simple and Rapid Test for Monitoring the Heat Evolution of Concrete Mixtures for Both Laboratory and Field Applications, FHWA DTF61-01-00042 (Project 17, Phase III), Final Report, 2008.
- [3] W.M. Hale, T.D. Bush, B.W. Russell, S.F. Freyne, Effect of curing temperature on hardened concrete properties, Transportation Research Record: Journal of the Transportation Research Board 1914 (2005) 97–104.
- [4] R.C. Tank, The rate constant model for strength development of concrete, Ph.D. Dissertation, Polytechnic University, Brooklyn, New York, 1988.
- [5] H.T. Yu, L. Khazanovich, M.I. Darter, A. Ardani, Analysis of concrete pavement responses to temperature and wheel loads measured from instrumented slabs, Transportation Research Record 1639 (1998) 94–101.
- [6] T. Nishizawa, T. Fukuda, S. Matsuno, K. Himeno, Curling stress equation for transverse joint edge of a concrete pavement slab based on finite-element method analysis, Transportation Research Record 1525 (1996) 35–43.
- [7] A.R. Mohamed, W. Hansen, Effect of nonlinear temperature gradient on curling stress in concrete pavements, Transportation Research Record: Journal of the Transportation Research Board 1568 (1997) 65–72.
- [8] C. Shi, R.L. Day, A calorimetric study of early hydration of alkali-slag cements, Cement and Concrete Research 25 (1995) 1333–1346.

- [9] M. Gawlicki, W. Nocuń-Wczelik, Łukasz Bąk, Calorimetry in the studies of cement hydration setting and hardening of Portland cement–calcium aluminate cement mixtures, *Journal of Thermal Analysis and Calorimetry* 100 (2010) 571–576.
- [10] J. Wang, P. Yan, H. Yu, Apparent activation energy of concrete in early age determined by adiabatic test, *Journal of Wuhan University of Technology—Materials Science Edition* 22 (2007) 537–541.
- [11] J.M. Ruiz, Q. Xu, Evaluation of time of set for concrete mixtures in cold weather with HIPERPAV Wisconsin model, Transportation Research Board, the 89th Annual Meeting Compendium of Papers DVD, Washington D.C. (2010).
- [12] Q. Xu, J. Hu, J.M. Ruiz, K. Wang, Z. Ge, Isothermal calorimetry tests and modeling of cement hydration parameters, *Thermochimica Acta* 499 (2010) 91–99.
- [13] D.P. Bentz, M.A. Peltz, J. Winpiger, Early-age properties of cement-based materials. II: Influence of water-to-cement ratio, *Journal of Materials in Civil Engineering* 21 (2009) 512–517.
- [14] M. Gerstig, L. Wadsö, A method based on isothermal calorimetry to quantify the influence of moisture on the hydration rate of young cement pastes, *Cement and Concrete Research* 40 (2010) 867–874.
- [15] I. Pane, W. Hansen, Investigation of blended cement hydration by isothermal calorimetry next term and thermal analysis, *Cement and Concrete Research* 35 (2005) 1155–1164.
- [16] L. Wadsö, An experimental comparison between isothermal calorimetry, semi adiabatic calorimetry and solution calorimetry for the study of cement hydration, Final Report, NORDTEST Project 1534-01, 2002.
- [17] P.F. Hansen, E.J. Pedersen, Maturity computer for controlling. Curing and hardening of concrete, *Nordisk Betong* 9 (1977) 21–25.
- [18] A.K. Schindler, Effect of temperature on hydration of cementitious materials, *ACI Materials Journal* 101 (2004) 72–81.
- [19] J.L. Poole, K.A. Riding, K.J. Folliard, M.C.G. Juenger, A.K. Schindler, Methods for calculating activation energy for Portland cement, *ACI Materials Journal* 104 (2007) 303–311.
- [20] K.O. Kjellsen, R.J. Detwiler, Later-age strength prediction by a modified maturity model, *ACI Materials Journal* 90 (1993) 220–227.
- [21] I. Pane, W. Hansen, Concrete hydration and mechanical properties under non-isothermal conditions, *ACI Materials Journal* 99 (2002) 534–542.
- [22] A.K. Schindler, Concrete hydration, temperature development, and setting at early ages, Doctoral Dissertation, The University of Texas at Austin, Austin, TX, 2002.
- [23] A.K. Schindler, K.J. Folliard, Heat of hydration models for cementitious materials, *ACI Materials Journal* 102 (2005) 24–33.
- [24] L. D'Aloia, G. Chanvillard, Determining the 'apparent' activation energy of concrete; E_a —numerical simulations of the heat of hydration of cement, *Cement and Concrete Research* 32 (2002) 1277–1289.
- [25] G. De Schutter, L. Taerwe, Degree of hydration-based description of mechanical properties of early-age concrete, *Materials and Structures* 29 (1996) 335–344.
- [26] Q. Xu, J.M. Ruiz, G.K. Chang, J.C. Dick, S.G. Garber, R.O. Rasmussen, HIPERPAV III: sensitivity analysis and moisture modeling, Federal Highway Administration Report, 2009.
- [27] Q. Xu, J.M. Ruiz, G.K. Chang, R. Rasmussen, D. Rozycki, A moisture transport model for enhancing FHWA HIPERPAV prediction, Transportation Research Record Journal of the Transportation Research Board 2113 (2009) 1–12.
- [28] J.M. Ruiz, P.K. Kim, A.K. Schindler, R.O. Rasmussen, Validation of HIPERPAV for prediction of early-age jointed concrete pavement behavior, Transportation Research Record Journal of the Transportation Research Board 1778 (2001) 17–25.
- [29] A.K. Schindler, J.M. Ruiz, R.O. Rasmussen, G.K. Chang, L.G. Wathne, Concrete pavement temperature prediction and case studies with the FHWA HIPERPAV models, *Cement and Concrete Composites* 26 (2004) 463–471.
- [30] W.J. Wilde, Computer-based guidelines for concrete pavements volume III—technical appendices, Federal Highway Administration Report FHWA-HRT-04-127, McLean, VA, 2005.
- [31] V. Rahhal, E. Talero, Influence of two different fly ashes on the hydration of portland cements, *Journal of Thermal Analysis and Calorimetry* 78 (2004) 191–205.
- [32] Y. Mostafa, P.W. Brown, Heat of hydration of high reactive pozzolans in blended cements: isothermal conduction calorimetry, *Thermochimica Acta* 435 (2005) 162–167.